JOURNAL OF EXPERIMENTAL AND THEORETICAL PHYSICS, 2024, Vol. 165, No. 3, pp. 413–426

ELECTRONIC PROPERTIES OF SOLIDS

THE ALLOYING EFFECT OF Si ON THERMODYNAMIC, MAGNETIC, AND ELASTIC PROPERTIES OF BCC Fe-Cr ALLOYS

© 2024 A. V. Ponomareva*

Materials Modeling and Development Laboratory, National University of Science and Technology 'MISIS', 119049, Moscow, Russia

**e-mail: alena.ponomareva@misis.ru*

Received July 04, 2023
Revised July 04, 2023
Accepted November 19, 2023

Abstract. In the framework of the density functional theory, the alloying effect of Si on the magnetic and elastic properties, as well as the thermodynamic stability at T = 0 K of ferromagnetic Fe-Cr solid solutions in the BCC structure was studied. Calculations of lattice parameters, mixing enthalpy, elastic constants, bulk moduli, Young's and shear moduli of disordered binary Fe-Cr and triple Fe-Cr-Si alloys containing 2.3 at. % and 4.7 at. % Si were performed using PAW-SQS and EMTO-CPA methods. Effective chemical interactions of the configuration Hamiltonian, magnetic characteristics and exchange interactions of the Heisenberg Hamiltonian are obtained. A comparative analysis of all obtained properties for ternary Fe-Cr-Si alloys with respect to binary Fe-Cr alloys is carried out. It was found that the addition of 2.3 at. % Si increases the thermodynamic stability of Fe-Cr alloys; this effect is enhanced with an increase in the silicon concentration to 4.7 at.%. The result is due to the Fe-Si and Cr-Si chemical interactions in addition to the magnetic Fe-Cr interactions that determine the stability of the diluted binary alloys. It is shown that with Si addition an increase in the elastic constant C_{44} is observed, the values of the constants C_{11}, C_{12} and elastic moduli are close to the corresponding values of binary Fe-Cr alloys. Analysis of the concentration dependence of the ductility parameter G/B and charge density difference maps allowed to establish correlations between the changes in interatomic bonding and the properties of the alloys.

Keywords: *Fe-Cr*, *alloying elements*, *silicon*, *thermodynamic and magnetic properties*, *elastic constants*, *ductility*, *first-principles calculations*

DOI: 10.31857/S00444510240311e3

1. INTRODUCTION

The Fe-Cr binary system is the basis for a large class of important technological materials. Fe-Cr alloys have a low swelling rate under the action of neutron irradiation, a low coefficient of thermal expansion, high thermal conductivity and strength at high temperatures, which makes it possible to use them, among other things, as materials for reactor vessels, containers for fuel compositions, cladding of fuel elements of active zones of thermal neutron reactors [1, 2].

Numerous studies have been devoted to the study of the properties of the Fe-Cr binary system. Currently, quantum mechanical calculations using density functional theory have made it possible to obtain reliable results of thermodynamic, mechanical, and magnetic properties of materials, and to predict the characteristics of complex systems. Theoretical studies of alloys based on the Fe-Cr system have allowed us to obtain a number of important conclusions and general patterns of the system, for example, on stability [3-7], interaction with defects [8-10], magnetic [5, 7, 11, 12] and elastic properties [13-16].

In [3-7], based on calculations of the enthalpy of formation of disordered Fe-Cr BCC alloys in the ferromagnetic state, the anomalous stability of the alloys at low chromium concentrations was found.

It has been shown that with an increase in the concentration of chromium, the enthalpy of formation becomes positive, passing through a maximum near the equiatomic composition. The concentration area with a chromium content of more than 20 at.% corresponds to alloys that undergo spinodal decompositionat a temperature of about 800 K, which negatively affects the mechanical properties of the system and requires a solution to neutralization of the negative result. In addition, since the range of negative values of enthalpy of formation in Fe-Cr alloys is quite narrow, increasing phase stability is also an urgent task.

Alloying is an effective method of improving the parameters of steels and alloys, including increasing mechanical characteristics and changing the boundaries of stability. For example, in theoretical works [11, 17, 18] it was shown that the addition of Ni, Mo, Mn reduces the stability of Fe—Cr alloys, while Al has a stabilizing effect. At the same time, it was concluded in [18] that at certain concentration combinations of Ni and Al in Fe-Cr-Ni-Al alloys, a simultaneous increase in their thermodynamic stability and ductility is predicted without a significant degradation in mechanical properties.

In this paper, the effect of silicon alloying on the properties of Fe—Cr alloys is studied. Silicon in steels and iron-based alloys is used as an alloying element capable of increasing crack resistance and corrosion resistance by forming a protective layer on the surface of the material. In [19], the corrosion behavior of $Fe - xCr - ySi$ ($x = 5,10$ at.% and $y = 5,10$ at.%) alloys at a temperature of 600° C in different gas mixtures with the same partial pressure of oxygen. The results of optical and scanning electron microscopy have shown that when the concentration of chromium is more than 5 at.% and 5-10 at.% silicon in the atmosphere of H_2–CO_2, an increase in oxide layers was observed, which significantly increased the corrosion resistance of the alloys. This is consistent with the data of [20], in which the authors observed that for Fe85Cr10Si5 alloy, high-temperature corrosion practically stops at temperatures of 870-1070 K. The results of the work [21] also demonstrated the beneficial effect of Si on the oxidation resistance of steels with 9 at.% Cr. The authors of [22] developed the interatomic potential (MEAM) for the Fe-Cr-Si system and obtained interaction profiles, structural and elastic characteristics for pure elements, binary compounds and for one composition Fe86Cr12Si2 (mass.%) commercial steel of the triple system, which is used as a high-temperature corrosion-resistant material. It is shown that the predicted properties using the developed potential are in good agreement with calculations within the framework of density function theory and available experimental data. The authors suggest that the developed potential can be applied as various applications, for example, for the design of multicomponent layered materials based on the Fe-Cr-Si system for operation under conditions of extreme temperatures and radiation doses.

In this paper, the thermodynamic, magnetic and elastic properties of BCC alloys of the triple Fe-Cr-Si system in a ferromagnetic state with a concentration of chromium $x_{Cr} = 0$–50 at.% and silicon concentration $x_{Si} = 2.3,4.7$ at.% are investigated. The values of lattice parameters, mixing enthalpies, elastic constants, bulk modules, Young's and shear modes, effective chemical pair interactions, magnetic characteristics and exchange interactions of the studied systems are obtained. Maps of the difference charge density were constructed, which made it possible to visualize the change in the atomic bond during alloying.

2. CALCULATION DETAILS

Ab initio modeling of the properties of Fe-Cr and Fe-Cr-Si systems was carried out at a temperature T = 0 K using projector augmented wave (PAW) methods [23, 24] implemented in the VASP [25-27] and exact muffin-tin orbitals (EMTO) in combination with the approximation a coherent potential (CPA) for modeling the substitution disorder [28, 29]. When using the PAW method, the atomic disorder of substitution alloys was modeled using the technique of special quasi-random structures (SQS) [30] on a 128-atomic BCC supercell. The cutting energy of the plane waves was chosen to be 500 eV. The Brillouin zone integration was performed using the Monkhorst-Pack special points method [31] on a 4x4x4 grid. To account for the exchange-correlation effects, a generalized gradient approximation with the PBE functional was used [32]. The convergence criterion of the electronic subsystem was chosen as 10^{-4} eV for the two subsequent iterations, and the ionic relaxation technique within the framework of the conjugate gradient method stopped when the forces were on the order of 10-3 eV/Å. The values parameters and the bulk modulus were obtained

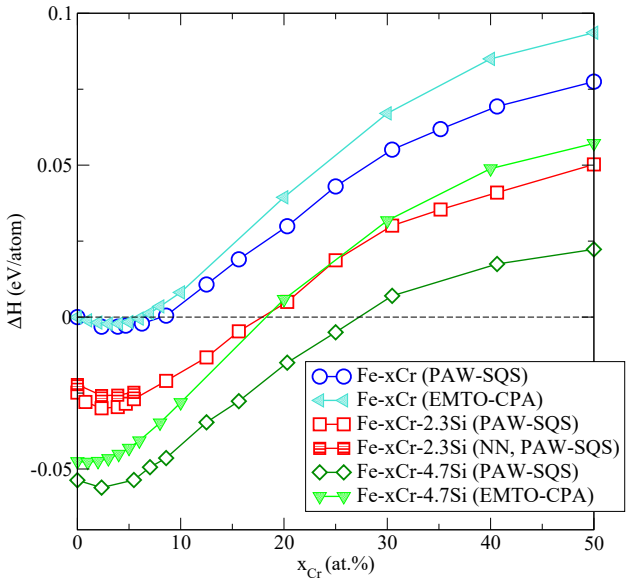

Fig. 1. (In color online) The mixing enthalpy of binary Fe-Cr and triple Fe-Cr-Si alloys, calculated using the PAW-SQS and EMTO-CPA methods

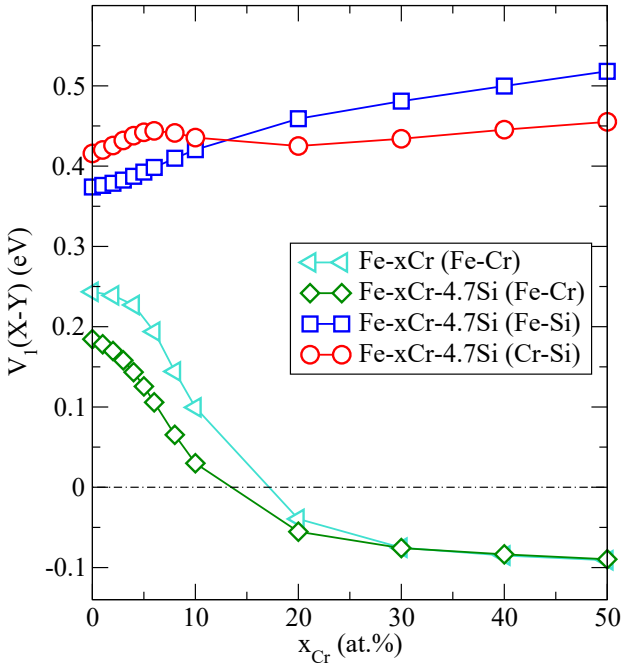

Fig. 2. (In color online) The parameters of binary (for Fe – *x*Cr) and quasi-binary (for Fe – *x*Cr – 4.7Si) pair interactions of the configuration Hamiltonian V_1 (X-Y) calculated by the EMTO-CPA method at the first CS

using regression according to the Birch–Murnaghan equation of state. Using the obtained values of the equilibrium parameters, the elastic coefficient C_{ij} was calculated using the stress-strain ratios, taking into account ±1% and ±2% relative deformations of the lattice. The values C_{11}, C_{12} and C_{44} would have been obtained by appropriate averaging [33] due to a decrease in lattice symmetry using SQS. The elastic modulus was obtained from the C_{ij} constants using Hill averaging for cubic crystals [34].

For EMTO calculations, the full charge density (FCD) [35] was represented by a single-center expansion of electron wave functions in terms spherical harmonics with orbital moments up to $l_{max} = 8$. Calculations were performed for the basic set, including valence *spdf* orbitals. Integration in the reciprocal space was carried out along a grid of $29 \times 29 \times 29$ k-points, energy integration was carried out in a complex plane using a semi-elliptical contour consisting of 24 points. The total energies are calculated using the generalized gradient approximation [32]. Effective pair interactions were determined in the ferromagnetic state using the screened generalize perturbation method (SGPM) [36, 37]. The screening constants necessary for calculating the electrostatic contribution to effective pair interactions were extracted from calculations on a 1024-atom supercell using the method of exact local self-consistent Green functions (ELSGF) [38]. The Bader charge analysis [39], obtained from the topological representation of the charge density distribution, was performed using the code developed in [40] for a grid $NG(X,Y,Z)F$ with a size of $400 \times 400 \times 400$.

3. RESULTS AND DISCUSSION

3.1. Thermodynamic properties and magnetic interactions

To assess the phase stability of Fe-Cr-Si ternary alloys containing 2.3 and 4.7 at.% silicon, consider the effect of silicon doping simultaneously on the mixing enthalpy of ΔH and the pair potentials $V_p(\mathrm{X}-\mathrm{Y})$ of the configuration Hamiltonian [41], since in a multicomponent alloy, the ΔH sign does not guarantee an unambiguous tendency to ordering or clustering. If in a multicomponent alloy the ΔH has negative values simultaneously with all positive quasi-binary values ΔH and the pair potentials $V_p(\mathrm{X}-\mathrm{Y})$, then this corresponds to the energy preference for the presence of pairs of unlike X – Y atoms at a distance of the radius of the coordination sphere p, which characterizes the tendency of the alloy to form a solid solution. If the ΔH has positive values and

at least one value of $V_p(\mathrm{X}-\mathrm{Y})$ is negative, then this is a sign that the alloy has a tendency to phase separation [42]. The calculated mixing enthalpy $\Delta H = E_{\mathrm{Fe}_{1-x-y}\mathrm{Cr}_x\mathrm{Si}_y} - (1-x-y)E_{\mathrm{Fe}} - xE_{\mathrm{Cr}} - yE_{\mathrm{Si}}$ of the studied alloys, where E_i are the total energies of the corresponding systems, are shown in Fig. 1. BCC-Fe in the ferromagnetic state, BCC-Cr in the nonmagnetic state, and Si in the diamond structure were used as the ground state. It should be noted that for Fe-Cr-Si alloys, points corresponding to the values of the ΔH Fe–Si alloys with silicon concentrations of 2.3 and 4.7 at.% are located on the y axis at zero chromium concentration.

In addition to the supercell method, in which a quasi-disordered periodic model (PAW-SQS) is used to describe the disordered structure, for alloys of the Fe-Cr-4.7Si system, the mixing enthalpy of ΔH was calculated using an approach based on the Green's function formalism, in which the substitution disorder is described in the coherent potential approximation (EMTO- CPA). The results of the two methods are compared in order to then extract effective pair $V_p(\mathrm{X}-\mathrm{Y})$ and exchange $J_p(\mathrm{X}-\mathrm{Y})$ interactions, which can be directly calculated using the EMTO-CPA method.

The graphs of the mixing enthalpy of binary $\mathrm{Fe}-x\mathrm{Cr}$ alloys for the two methods are in good agreement with each other (Fig. 1), while fully reproducing the region of anomalous stability at low chromium concentration obtained in previous studies using PAW, EMTO, ELSGF methods [3-7], which show an interval of negative values ΔH and the presence of a minimum on the curve with a low chromium content. The concentration of chromium corresponding to the minimum depends on the method and ranges from 3 to 10 at.%. In this case, the curves obtained by both methods have minima at $x \approx 4$ at.% Cr, while using the EMTO-CPA method, the ΔH values become positive at $x \approx 6$ at.% Cr, and in the PAW-SQS method, the ΔH curve lies below the EMTO graph, has a flatter region of minimum values and crosses the x axis at about 9 at.% chromium. With an increase in chromium concentration, the values of ΔH become positive and increase with an increase in x, the values of the EMTO-CPA method show a more dramatic increase than the values obtained by the PAW-SQS method. The observed difference in the results of the two methods may be a consequence of the consideration in the PAW-SQS method of lattice relaxation and the effect of the local environment in this system, the presence of which will be demonstrated below.

Adding 2.3 at.% silicon shifts the point with zero chromium concentration to the range of negative values up to -0.028 eV (in the PAW-SQS method). With an increase in the chromium concentration, the type of ΔH for $\mathrm{Fe}-x\mathrm{Cr}-2.3\mathrm{Si}$ alloys is similar to the Fe–Cr-dependence, while an increase in the depth of the minimum and its shift towards a lower chromium concentration is observed, however, due to a shift to zero of the chromium concentration, the region of negative values of the mixing enthalpy increases from 9 up to 18 at.% Cr. The shift of the ΔH for Fe-2.3Si alloy to negative energies is qualitatively consistent with the results of the study of the Mossbauer spectrum on ^{57}Fe nuclei at room temperature for Fe-Si alloys [43]. In the work, the value of the energy of dissolution of the Si impurity in the Fe BCC was obtained, equal to -0.38 eV/atom, i.e., the process of dissolution of the impurity corresponds to exothermic reaction, which does not contradict the results of this study. Increasing the silicon concentration to 4.7 at.% shifts the point $x_{\mathrm{Cr}} = 0$ even more to -0.054 eV (-0.048 eV) in the PAW-SQS (EMTO-CPA) method, while the range of positive enthalpy values increases to 25 at.% Cr (18 at.%).

In [5], it was established that there is a repulsion between Cr atoms in a binary Fe-Cr system at $x_{\mathrm{Cr}} < 12$ at.%, which is strong for the nearest neighbors, significant at least up to the sixth coordination sphere (CS) of the central atom and has a magnetic origin. The appearance of Cr atoms as the nearest neighbors increased the enthalpy of formation by values up to 10 MeV/atom. In order to find out the presence of a tendency to clustering at Si concentrations in Fe-Cr-Si alloys, calculations were performed for $\mathrm{Fe}-x\mathrm{Cr}-2.3\mathrm{Si}$ alloys in the region of stability with a chromium concentration of 0, 2.3, 3.90, 5.47 at.%, in which Si atoms are located only in the 1-2 CS of each other. For all chromium concentrations, the energies of such alloys were higher (by about 5 MeV/atom) than for the disordered solid solution (Fig. 1). This is consistent with the analysis of the binding energy values between two Si atoms in Fe-Si alloys carried out in [43], which showed that the interaction between Si atoms in the studied materials is repulsive.

Therefore, further studies were carried out on SQS cells with Warren-Cowley short-range parameters [44] close to zero to 4 CS, which corresponds to an disordered state.

Using Fig. 2, we consider the behavior of effective pair cluster interactions of the nearest neighbors of the $V_1(\mathrm{X}-\mathrm{Y})$ Hamiltonian

$$H_{conf} = -\frac{1}{2}\sum_{p}\sum_{\mathrm{X}\neq\mathrm{Y}} V_p(\mathrm{X}-\mathrm{Y})\sum_{i,j\in p}\delta c_i^{\mathrm{X}}\delta c_j^{\mathrm{Y}},$$

where δc_i^{X} is the fluctuation of the concentration of component X at position i from its average concentration in the alloy. The values of $V_1(\mathrm{X}-\mathrm{Y})$ in the EMTO-CPA method have a quasi-binary representation, the advantage of which is its direct connection with Hamiltonian and interactions of binary systems of components that are part of a multicomponent system [41]. The values $V_1(\mathrm{X}-\mathrm{Y})$ were obtained for ferromagnetic alloys with a fixed silicon concentration $x_{\mathrm{Si}} = 4.7$ at.% for the equilibrium volumes at each concentration point. As can be seen in Fig. 2 and demonstrated in previous studies [7, 11, 45], dilute binary Fe-Cr alloys have positive values of effective interatomic interactions at the first CS, which indicates a tendency to form a solid solution. This result is consistent with the negative calculated values of the mixing enthalpy of Fe-Cr alloys. With an increase in the concentration of chromium to about 18 at.% pair interactions change sign, demonstrating the appearance of a tendency to clusterization in the system, which correlates with positive values of ΔH. The inversion of the short-range order parameters was theoretically predicted using the generalized perturbation method (GPM) [46] and subsequently confirmed by measurements of diffuse neutron scattering [47] and the Mossbauer atomic short-range order study (ASRO) [48].

In $\mathrm{Fe}-x\mathrm{Cr}-4.7\mathrm{Si}$ alloys, Fe-Cr interactions decrease relative to binary alloys and the chromium concentration decreases (from about 18 to 15 at.% Cr), at which a change in the sign of interactions is observed. However, Fe-Si and Cr-Si interactions appear in ternary alloys, which have positive values and exceed Fe-Cr interactions in magnitude. The high values of $V_1(\mathrm{Fe}-\mathrm{Si})$ coincide with the values of the pair Fe-Si potentials for an alloy with 8 at.% Si obtained in [49], in which the role of magnetism in the formation of short-range order in Fe-Si alloys was investigated. At zero and low concentrations of chromium, the pair Fe-Si and Cr-Si interactions make a significant contribution to the configuration Hamiltonian [7, 45], which stabilizes the system. Cr-Si interactions also increase the depth of the minimum, which leads to a shift towards high concentrations of chromium, at which the ΔH value is negative. However, with an increase in chromium concentration, the role of Fe-Cr interactions increases, and their negative values after inversion increase the tendency to phase separation. Thus, in the range of chromium concentrations from 0 to 20 at.% for alloys containing 4.7 at.% Si, all pair interactions have positive values, and the mixing enthalpy is negative, which shows the presence of a tendency in the system to form a solid solution.

Next, we will analyze the concentration changes in the lattice parameters and magnetic moments of Fe-Cr-Si alloys, which are shown in Fig. 3. The dependences of the lattice parameters in Fe-Cr and Fe-Cr-Si alloys are nonlinear with positive deviations from Vegard's law with a maximum of about 10 at.%, while the curves of the Si lattice parameters almost repeat the shape of the curve corresponding to Fe-Cr alloys. Relative to pure iron, the addition of Si almost does not change the lattice parameter, with the appearance and increase of chromium content, the concentration dependences of Fe-Cr-Si alloys lie below the Fe-Cr curve, while the higher the concentration of silicon, the smaller the lattice parameters. For Fe-Cr alloys, the deviation of lattice parameter values from experimental data is about 1% (see Table 1 and papers [50, 51]), which can be explained by the generalized gradient approximation used, which, as is known, underestimates the equilibrium volume of magnetic 3*d* metals [52]. But, as shown in [16], the use of experimental lattice parameters to calculate elastic properties in Fe-Cr alloys does not change their dependencies relative to the calculated lattice parameters, leading only to certain shifts depending on the property under consideration.

On all curves, at low concentrations of chromium, a sharp increase in the lattice parameters indicates a relatively large effective size of the Cr atom in dilute Fe-Cr alloys. As the chromium content increases, the slope of the curve changes, which corresponds to a decrease in the effective size of Cr atoms. At the same time, the addition of silicon reduces the size of the chromium atom at the intervals of both growth and decline of the lattice parameter values.

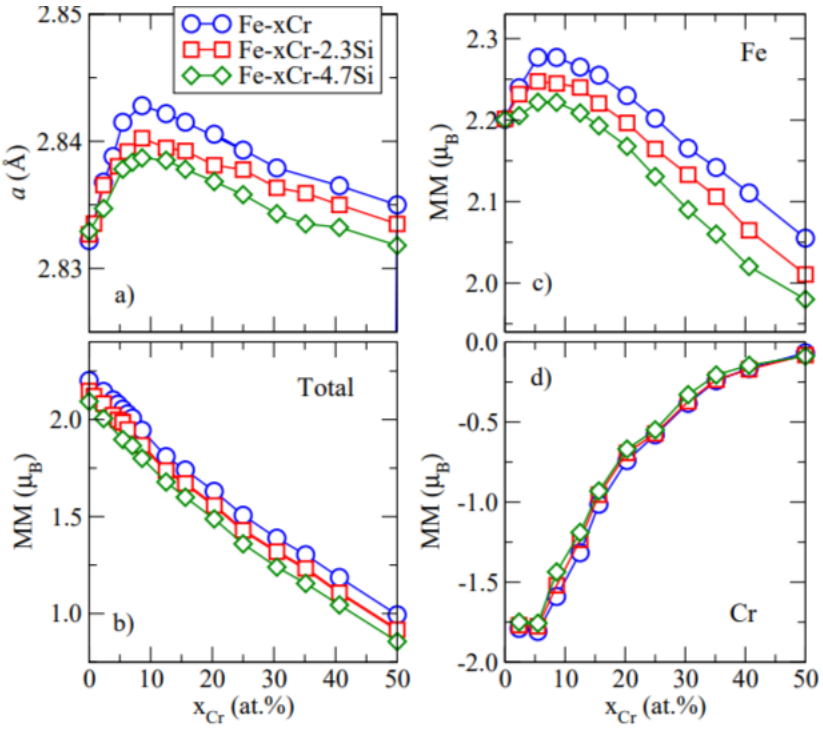

Fig. 3. (In color online) Lattice parameters (*a*) and magnetic moments (*b*-*d*) of binary Fe-Cr and triple Fe-Cr-Si alloys calculated using the PAW-SQS method

As shown by the calculation of Bader charges Q_B^X, this is due to the charge transfer from chromium atoms mainly to silicon atoms and to a lesser extent to iron atoms. Iron atoms with a deficiency of electrons, surrounded by silicon, have also been found. So, for the $Fe-12.5Cr-4.7Si$ alloy, the following values change: Q_B^{Cr} from about -0.34e to -0.43e, Q_B^{Si} from about +0.16e to +0.26e, Q_B^{Fe} from about -0.04e to +0.15e, where e is the electron charge. It is worth noting that the signs and values of Q_B^X correlate with the values of the electro-negatives of the alloy elements.

Let's consider the magnetic characteristics of the studied systems (Fig. 3 and 4). The total magnetic moments in binary alloys decrease with an increase in the chromium content. When silicon is added, all concentration curves lie lower than the Fe-Cr dependence, but the difference in values is no more than $0.1\,\mu_B$ in dilute alloys and about $0.2\,\mu_B$ in alloys with a chromium concentration at approximately 50 at.%. The average magnetic moments of Fe and Cr atoms also decrease with increasing concentrations of chromium and silicon, but the change in the magnetic moments of iron is significantly weaker.

There are regions with small extremes on the curves for all Fe-Cr and Fe-Cr-Si alloys, while the maximum is more pronounced for the graph of magnetic moments of Fe atoms, the behavior of which resembles the concentration dependence of the lattice parameters. The magnetic moment of the iron atom is parallel to the full magnetization vector, the negative sign of the magnetic moment of the Cr atom reflects the fact that in the ferromagnetic state, the magnetic moments of chromium atoms are antiparallel to the magnetic moments of iron atoms and the full magnetization vector. With an increase in the chromium concentration, the values of the magnetic moments of chromium decrease sharply, reaching zero at approximately 50 at.%.

The local magnetic moments of all atoms in Fe-Cr and Fe-Cr-Si alloys are shown in Fig. 4, from which it follows that in the magnitudes of the magnetic moments of Fe and Cr there is a spread of values, especially for chromium atoms. At the same time, the values of the local and, accordingly, the

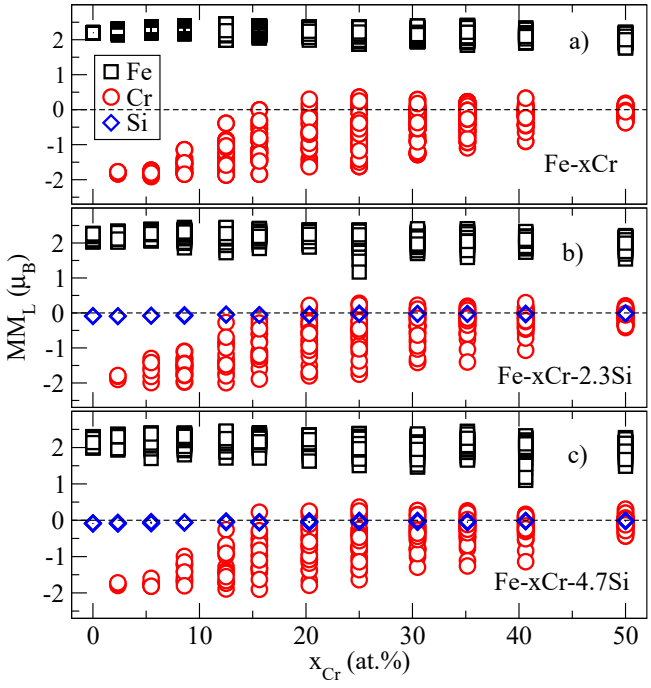

Fig.4. (Online in colour) Values of local magnetic moments of Fe, Cr, Si atoms in binary Fe-Cr and triple Fe-Cr-Si alloys calculated using the PAW-SQS method

average magnetic moments of Si atoms are close to zero for all the alloys under consideration.

The magnetic moments of iron atoms have a range of values for the studied systems and concentration ranges from 1.1 μ_B to 2.4 μ_B. Fe atoms with minimal magnetic moments of about $(1.1-1.5)\mu_B$ are observed in Fe-Cr-Si alloys with a chromium concentration of 25-40 at.% (Fig. 4 *b*, *c*) and contain 1-2 CS 2 silicon atoms and 4-5 chromium atoms. Si atoms in 1 CS of iron reduce the magnetic moment of the latter from about $(0.1-0.2)\mu_B$ (1 Si atom) to $0.3\mu_B$ (2 Si atoms), Cr atoms also reduce the magnetic moment on iron atoms, but to a lesser extent than silicon. The maximum values on iron atoms are observed in situations when 1 CS is filled with only iron atoms or chromium atoms with high antiferromagnetic values of magnetic moments are present in it, which, as will be shown below, satisfy the sign of the Fe-Cr exchange interaction. The dependence of the magnetic moment of an iron atom on the number of neighboring silicon atoms is consistent with the results of experimental work [53], in which, when studying macroscopic and local atomic structures, as well as the magnetic characteristics of crystalline and amorphous Fe-Si alloys, it was demonstrated that a decrease in the number of neighboring Fe atoms due to their substitution two or more Si atoms leads to a significant decrease in the local magnetic moment of the Fe atom. Also in [54], when measuring the fields of ultrafine interaction in Fe_3Si with the DO_3 structure, it was found that the magnetic moment of an atom with eight iron atoms in its 1 CS has a magnetic moment equal to $2.2\mu_B$, at the same time an atom of Fe with four iron atoms and four silicon atoms in 1 CS have a magnetic moment equal to $1.2\mu_B$.

The magnetic moments of chromium atoms have a range of values for the studied concentration range from $-1.9\mu_B$ to $0.3\mu_B$. For a binary Fe-Cr alloy, it was shown in [5] that the values of the magnetic moment Cr strongly depend on the local environment. This is also confirmed by these calculations (Fig. 4a). At low concentrations of chromium (0-5 at.%) magnetic moments have values at measured $(1.8\pm0.1)\mu_B$, with increasing concentration, the spread increases and some magnetic moments begin to decrease. This is observed on chromium atoms, which are the nearest neighbors of each other, i.e. the magnetic moments of chromium atoms, which are surrounded by iron atoms, remain high, and those in which chromium atoms appear in 1 CS begin to decrease (Fig. 4, chromium concentrations from about 15 to 30 at.%). With an increase in the concentration of chromium, such atoms associated with the atoms of the same name become more and more, and at $x_{Cr}\approx 50$ at.%, the magnetic moments on chromium atoms become zero (Fig. 4). It should also be noted that the magnitude of the magnetic moment of chromium decreases if chromium atoms are present in the second CS, even if only iron atoms are present in the first; this decrease is less than when located in 1 CS, but also linearly depends on the number of Cr atoms.

When silicon is added, the dependence of the magnetic moments of chromium on the number of neighbors of the same name is completely preserved, in addition to the dependence on the presence of Si atoms. It was found that at a fixed concentration, the magnetic moment of a chromium atom is maximum when its 1 and 2 CS are completely occupied by iron atoms, as well as if there are silicon atoms in 1 CS under the condition that only iron atoms are placed in the remaining positions in 1-2 CS. The value of the magnetic moment of Cr atoms next to silicon at some positions is even higher than when

completely surrounded by iron atoms. When chromium atoms appear, the magnetic moment decreases sharply, as in the case of binary alloys, but in the presence of a silicon atom in the first CS of chromium with several atoms of the same name, it allows you to keep the magnetic moment at the level of values when 1-2 chromium atoms are less in 1 CS.

A strong change in the magnetic moment of chromium in the presence of the like neighbors in alloys based on the Fe-Cr system is associated with the behavior of magnetic exchange interactions $J_1(\mathrm{X}-\mathrm{Y})$ between atoms X and Y at 1 CS Heisenberg Hamiltonian [55]

$$H_{magn} = -\sum_{p}\sum_{i,j\in p} J_p(\mathrm{X}-\mathrm{Y})e_i \cdot e_j,$$

where p is the number of CS, $\mathbf{e}_i$ is the unit vector in the direction of the magnetic moment at node i. As shown in [5, 7, 45] and in Fig. 5, in binary alloys, the values of the interactions J_1 (Cr-Cr) and J_1 (Fe-Cr) are negative, J_1 (Fe-Fe) are positive, i.e. Cr atoms interact antiferromagnetically with each other and with iron atoms, at the same time, ferromagnetic interaction is established between iron atoms. Therefore, the appearance of a pair of chromium atoms as the nearest neighbors causes magnetic frustration, leading to a gradual loss of the magnetic moment on the chromium atom with an increase in x_{Cr} [5]. When silicon is added, the exchange interactions do not change fundamentally: J_1(Si-X) are almost equal to zero, while Fe-Cr interactions remain dominant at low chromium concentrations, and at high concentrations — J_1(Fe-Fe). There is a slight decrease in Fe-Cr and Fe-Fe values and a slight increase in Cr-Cr interactions, a weak increase in J_1(Cr-Cr) relative to the binary alloy correlates with a slight increase in the magnetic moment on the chromium atom near the silicon atom. Therefore, with an increase in chromium concentration, the occurrence of frustrated states in ternary alloys also leads to a gradual degradation of the magnetic moment on chromium atoms, but slightly slower than in the binary system.

To analyze the relationship between magnetic interactions and phase stability, it is worth noting that in [45], in which the exchange interactions were considered as part of the configuration of Hamiltonian, it was shown that in Fe-Cr alloys, the magnetic interactions J_1 (Fe-Fe) and J_1(Cr-Cr) contribute

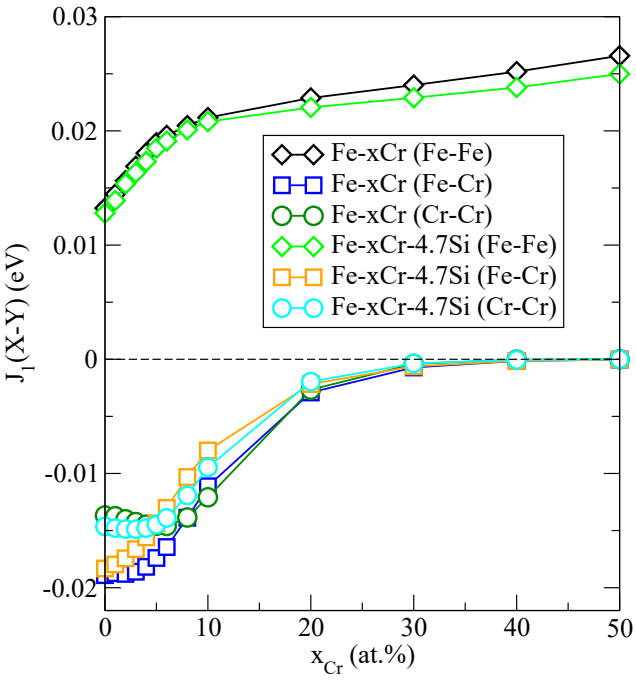

Fig. 5. (In color online) The parameters of the exchange interaction of the Heisenberg Hamiltonian $J_1(\mathrm{X}-\mathrm{Y})$ at the first CS in binary Fe – xCr and triple Fe – xCr – 4.7Si alloys calculated using the EMTO-CPA method

to solid solution formation, and J_1(Fe-Fe) clustering in this system. In addition, at low chromium concentrations, the exchange interactions of Fe-Fe and Cr-Cr largely compensate for each other, and the exchange interactions of Fe-Cr are the dominant contribution to the effective cluster interactions of V_1(X-Y), which determines the stability of the alloy, manifested in negative values of the enthalpy of binary Fe–Cr alloys [45] (see Fig. 1). An increase in chromium concentration and the loss of magnetic moments by chromium atoms leads to a decrease in magnetic and chemical interactions between Fe and Cr atoms, while the Fe-Fe interaction becomes dominant, which leads to destabilization of the alloy. Since the exchange interactions change insignificantly with the addition of silicon, it can be concluded that the stabilization of Fe-Cr-Si alloys (relative to Fe-Cr alloys) is influenced by the chemical interactions of V_1(Fe-Si) and V_1(Cr-Si) in addition to the magnetic interactions of Fe-Cr, which determine the stability of dilute binary Fe-Cr alloys.

The features of the electronic structure of the studied alloys are also related to the dependence of the values of the magnetic moment of chromium atoms

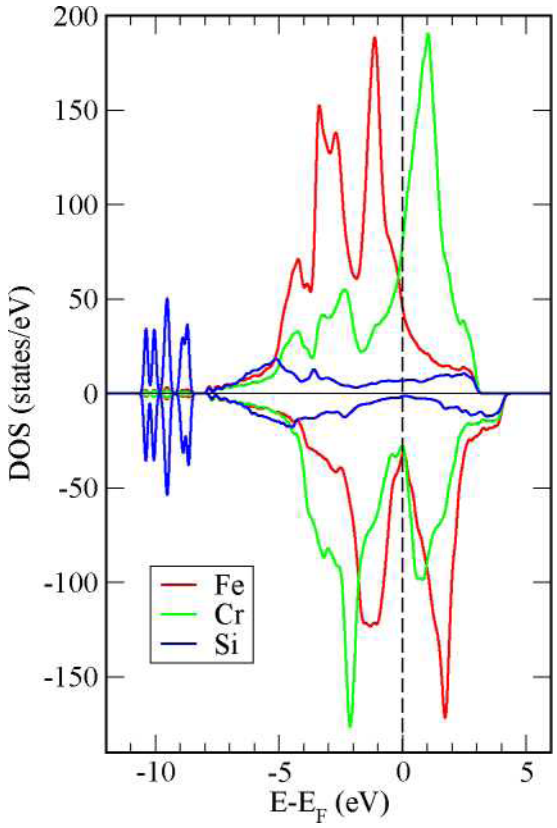

Fig. 6. (In color online) The local density of electron states in the ferromagnetic BCC alloy Fe-8.6Cr-4.7Si obtained using the PAW-SQS method

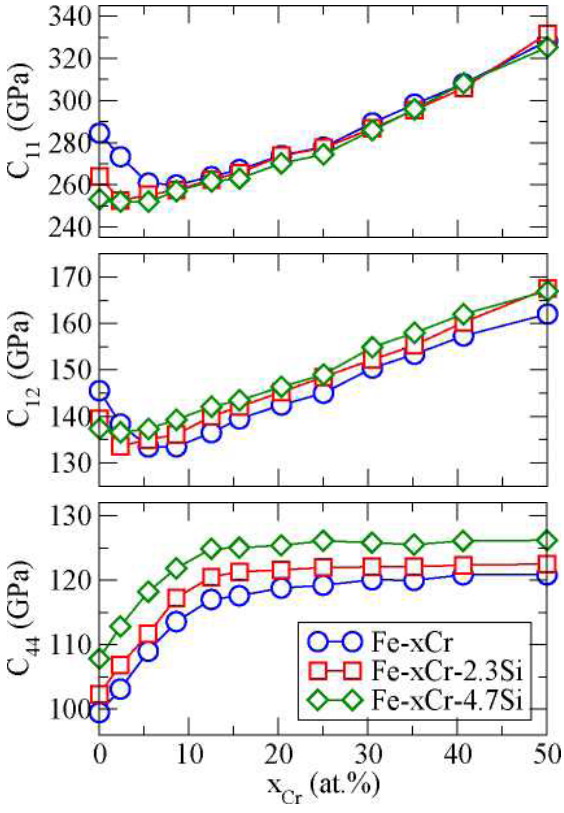

Fig. 7. (In color online) Elastic constants C_{11} , C_{12} , C_{44} of binary Fe-Cr and triple Fe-Cr-Si alloys calculated using the PAW-SQS method

on the environment. In both binary Fe-Cr [7,11] and triple Fe-Cr-Si systems (Fig. 6), at low concentrations of chromium, the density of electronic states (DOS) shows a different filling of the *d*-band with the spin up of iron and chromium atoms. Iron has an almost completely filled band with spin up, while chromium has partially unfilled antibonding states, which may be the cause of fluctuations in magnetic moments due to the effect of the local atomic environment [56]. At the same time, in the DOS band with spin down, the Fermi energy is in the pseudo-gap for both the Fe atom and the Cr atom. As noted above, the addition of silicon causes charge transfer from chromium and iron atoms to silicon atoms. When doped with silicon, both DOS bands are rearranged, associated with the formation of *s–d* (in the range from -11 to -9 eV) and *p–d* (-7 to -4 eV) hybridization of Fe and Cr states with Si states (Fig. 6). There is also an electron outflow and a decrease in DOS in the spin-up band (relative to the general magnetization vector), since it is energetically favorable to fix the Fermi energy in a pseudo-gap. This leads to a decrease in the magnetic moment on iron atoms next to silicon and, conversely, to an increase in the magnetic moment on chromium atoms located in 1 CS of silicon atoms.

3.2. Elastic properties

The strength characteristics of the material, as well as its mechanical properties, are related to the values of elastic constants, which, in turn, carry important information about microscopic interatomic interactions. Figures 7 and 8 show the elastic constants C_{ij}, polycrystalline modules obtained by the Hill method, as well as the ratio of shear and bulk moduli, *G/B*, for binary and ternary alloys as a function of chromium concentration. The elastic properties of the alloys were investigated using the PAW-SQS method for calculated equilibrium lattice parameters with optimized atomic positions and cell shapes with appropriate averaging along the axes [33] due to a decrease in lattice symmetry when using SQS.

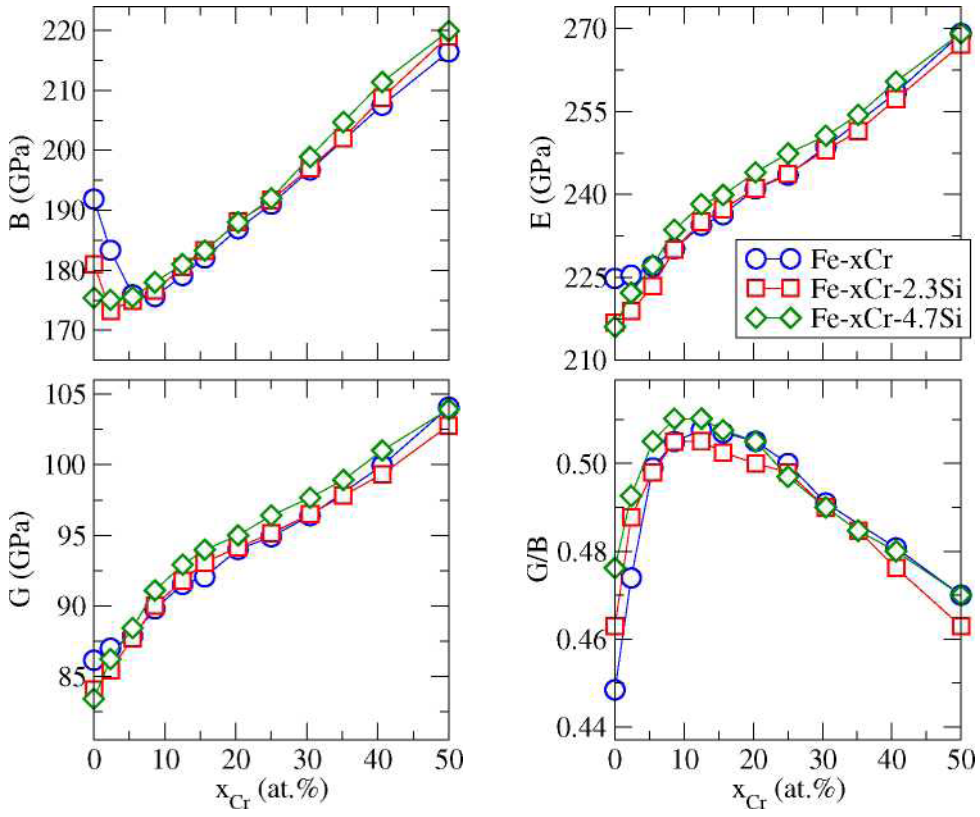

Fig. 8. (In color online) The bulk modulus B, the Young's modulus E, the shear modulus G and the G/B ratio for binary Fe-Cr and triple Fe-Cr-Si alloys calculated using the PAW-SQS method

Fig. 7 shows that the elastic constants C_{11} and C_{12} for dilute binary and ternary alloys have shallow minima of about 5-7 at.% Cr, and at $x_{Cr} > 10$ at.% there is an increase in these conditions. For Si alloys, the minimum depth decreases relative to the values for the Fe-Cr system, at low chromium concentrations up to 10 at.% all values of C_{11} and C_{12} are slightly lower than values for Fe—Cr alloys. With an increase in the concentration of chromium, the constants increase, practically falling with each other; a slight increase in C_{12} for alloys with Si is observed relative to Fe-Cr alloys. The C_{44} constant for all alloys increases to 15 at.% Cr, at $x_{Cr} > 15$ at.% the dependences reach a plateau, while the values for alloys with 2.3 at.% Si lie slightly higher than the values for binary alloys, the highest constants have Fe-xCr-4.7Si alloys for the entire chromium concentration range under study.

Bulk modules in Fe-Cr alloys have a nonmonotonic concentration dependence with a local minimum at 10 at.% Cr, which correlates with a change in lattice parameters. When Si is added, the nonmonotonicity decreases, while at very low values of x_{Cr}, the values of the bulk modulus B are lower than in the binary alloy (despite the fact that the lattice parameter decreases with increasing silicon concentration), with increasing chromium concentration, the values for Fe-Cr and Fe-Cr-Si alloys they practically match. The values of Young's modulus E and shear modulus G in triple alloys are very close to the values in binary alloys with a slight decrease in the region of dilute compositions. The values of the modules show reasonable agreement with the experimental results for Fe—Cr alloys, the theoretical values are slightly higher due to underestimation of the lattice parameters. At the same time, the main trends in changing properties with increasing chromium concentration are well reproduced: the experimental volumetric module also has a minimum, and $\Delta E/\Delta x_{Cr}$ and $\Delta G/\Delta x_{Cr}$ have positive values (see [57] and the table). It is worth noting that all the stability criteria of cubic crystals, $C_{44} > 0$, $C_{11} - C_{12} > 0$, $C_{11} + 2C_{12} > 0$ [58], are satisfied for both binary and ternary alloys.

Let's analyze the change in the G/B ratio during alloying (Fig. 8). It was shown in [59] that the G/B ratio can be used as an indicator of plastic ($G/B < 0.5$) or brittle behavior ($G/B > 0.5$), while the higher the G/B value, the more brittle the material

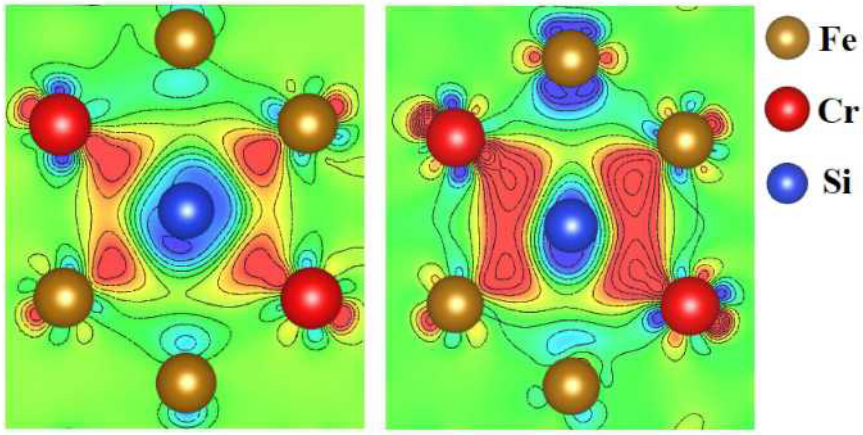

Fig. 9. (In color online) The difference charge density of Fe-5.4Cr-4.7Si and Fe-30.5Cr-4.7Si alloys, calculated using the PAW-SQS method. The red color indicates an excess charge, the blue color indicates a defciency of electrons

is. Fig. 8 shows that the dependences of G/B on the chromium concentration of all alloys have a strongly nonlinear character with a pronounced maximum at concentrations of about 10 at.%, i.e., at the same concentrations where the maximum curves of lattice parameters and magnetic moments of iron atoms are located. A sharp increase in G/B at low x_{Cr} indicates the formation of directional bonds with a high degree of covalence, which correlates with large magnetic moments on Fe and Cr atoms with localized valence electrons. With increasing x_{Cr} the magnetic moments on the chromium atom decrease (see Fig. 4), which leads to the appearance of delocalized electrons capable of participating in atomic bonding. Indeed, the ratio of G/B at $x_{Cr} > 10$ at. % begins to decrease sharply, which indicates an increase in the degree of metallicity of the bond, which ensures an increase in C_{ij} and elastic moduli.

When silicon is added, the dependencies C_{44} in Fig. 7 follow the reverse order of the lattice parameters (see Fig. 3), which is to be expected. However, the bulk modulus B and the constant C_{11} in Fe-Cr—Si alloys decrease at low x_{Cr} relative to the values in Fe—Cr alloys. At the same time, the G/B ratio for ternary alloys is higher than for binary alloys. This may indicate an additional restructuring of the charge density due to the presence of silicon, which leads to a weakening of the axial atomic bond and an increase in the atomic bond responsible for shear deformations.

Table 1. Experimental values of the parameters of the lattice a, Young's modulus E, shear modulus G, bulk modulus B and the ratio G/B for some BCC alloys Fe-Cr and Fe-Cr-Si

System,	a,	E,	G,	B,	G / B
concentration, at.%	Å	GPa	GPa	GPa	
Fe–1.98Cr [50]	2.869				
Fe–3.35Cr [50]	2.870				
Fe–5.48Cr [50]	2.871				
Fe–1.65Cr [57]		209	80.9	167.8	0.48
Fe–5.56Cr [57]		211	82.4	161.4	0.51
Fe–10.7Cr [57]		215	84.5	157.1	0.51
Fe–14Cr–3Si [60]		178	68	157	
Fe–10Cr–5Si [61]	2.869				

To verify this, a calculation of the difference electron density was carried out for the Fe-5.4Cr-4.7Si and Fe-30.5Cr-4.7Si triple alloys as $\Delta\rho = \Delta\rho_{Fe-Cr-Si} - \Delta\rho_{Fe-Cr} - \Delta\rho_{Si}$ (Fig. 9), which allowed us to isolate the direct influence of silicon. Figure 9 clearly shows areas with an excess of electrons forming on the Si-Cr and Si-Fe bond lines, which is consistent with the calculation of Bader charges. The maximum localization of the excess charge is observed in the direction of the nearest neighbor, which indicates an increase in the shear component of the atomic bond and is confirmed by an increase in the elastic constant C_{44} (see Fig. 7).

With an increase in chromium concentration, electron delocalization increases significantly (due to a decrease in the magnetic moment on chromium atoms) and the formation of regions with excess charge can be observed not only between the first Si-Fe- and Si-Cr-neighbors, but also between the second Fe-Cr-neighbors, which strengthens the axial coupling and leads to an increase in the constant C_{11} and the modules B , E and G.

4. CONCLUSION

In this paper, within the framework of the *ab initio* approach using PAW-SQS and EMTO-CPA methods, the effect of Si alloying on the thermodynamic stability, magnetic and elastic properties of ferromagnetic Fe-Cr solid solutions in the BCC structure is investigated. It is demonstrated that calculations for Fe-Cr alloys reproduce the region of the negative values of the mixing enthalpy of ΔH and show a minimum on the curve at a low chromium content, which reflects the anomalous stability of ferromagnetic dilute binary alloys found in previous studies [3-7]. When adding 2.3 at.% of silicon, there is an increase in the depth of the minimum on the enthalpy curve and an increase in the region of negative values of the mixing enthalpy compared to the binary system. When the silicon concentration increases to 4.7 at.%, this effect is enhanced. At the same time, in the range of chromium concentrations from 0 to about 20 at.% for alloys containing 4.7 at.% Si, all pair interactions V_1 (X-Y) have positive values, which, together with negative values of the mixing enthalpy, demonstrate tendency to form a solid solution in the system. Analyzing the trends in the dependence of the mixing enthalpy of ΔH, pair potentials V_1 (X-Y), exchange interactions J_1(X-Y) in binary and triple alloys, it can be concluded that the addition of Si to Fe-Cr alloys increases the solubility of Cr in ferromagnetic iron, for which Fe-Si and Cr-Si chemical interactions are responsible in addition to the magnetic interactions of Fe-Cr, which determine the stability of dilute binary alloys.

In the Fe-Cr-Si system, at low concentrations of chromium and silicon, the presence of weak repulsion of Si atoms located in the first and second coordination spheres of each other is shown.

It was found that in ternary alloys, with an increase in the chromium content, the tendency of a gradual decrease in magnetic moments on chromium atoms due to magnetic frustrations persists. At the same time, the values of the magnetic moments of iron atoms next to silicon decrease, and chromium atoms increase, which is associated with the electronic structure of ferromagnetic BCC alloys based on the Fe-Cr system.

It is shown that the elastic constants C_{11}, C_{12} and the bulk modulus B for dilute binary Fe-Cr and triple Fe-Cr-Si alloys have shallow minima at x_{Cr} = 5-7 at.%, and at $x_{Cr} > 10$ at.% there is an increase in these elastic constants. Over the entire concentration range considered, the values of C_{11} , C_{12} , the bulk modulus B, the Young modulus E and the shear modulus G for triple alloys are very close to the corresponding values for binary alloys. The constants C_{44} for all alloys increase up to ~15 at.% Cr, at xCr > 15 at.% the dependences show a weak increase, while the C_{44} values for ternary alloys are higher than for binary ones.

The analysis of the parameters of the ductile behavior of G/B and maps of the difference charge density allowed us to establish the relationship between the elastic and magnetic properties of alloys and the redistribution of electron density during alloying. It is shown that with an increase in the chromium concentration in ternary alloys, a change in the ratio of the atomic bond components is observed with a decrease in the proportion of covalence and an increase in the degree of metallicity due to electron delocalization.

FUNDING

The work was carried out with the support of the Russian Science Foundation (project No. 22 12-00193).

REFERENCES

1. A. A. F. Tavassoli, Journal of Nuclear Materials 258–263, 85 (1998).
2. K. L. Murty and I. Charit, Journal of Nuclear Materials 383, 189 (2008).
3. P. Olsson, I. A. Abrikosov, L. Vitos, and J. Wallenius, Journal of Nuclear Materials 321, 84 (2003).
4. P. Olsson, I. A. Abrikosov, and J. Wallenius, Phys Rev B 73, 104416 (2006).
5. T. P. C. Klaver, R. Drautz, and M. W. Finnis, Phys Rev B 74, 094435 (2006).
6. M. Yu. Lavrentiev, R. Drautz, D. Nguyen-Manh, T. P. C. Klaver, and S. L. Dudarev, Phys. Rev. B 75, 014208 (2007).
7. P. A. Korzhavyi, A. V. Ruban, J. Odqvist, J.-O. Nilsson, and B. Johansson, Phys Rev B 79, 054202 (2009).
8. J. S. Wróbel, M. R. Zemła, D. Nguyen-Manh, P. Olsson, L. Messina, C. Domain,
9. T. Wejrzanowski, and S. L. Dudarev, Comput Mater Sci 194, 110435 (2021).
10. P. Olsson, C. Domain, and J. Wallenius, Phys Rev B 75, 014110 (2007).
11. L. Messina, T. Schuler, M. Nastar, M.-C. Marinica, and P. Olsson, Acta Mater 191, 166 (2020).
12. A. V. Ponomareva, A. V. Ruban, B. O. Mukhamedov, and I. A. Abrikosov, Acta Mater 150, 117 (2018).
13. I. K. Razumov and Yu. N. Gornostyrev, Physics of Metals and Metallography 122, 1031 (2021).
14. X. Li, X. Li, S. Schönecker, R. Li, J. Zhao, and L. Vitos, Mater Des 146, 260 (2018).
15. H. Zhang, M. P. J. Punkkinen, B. Johansson, S. Hertzman, and L. Vitos, Phys Rev B 81, 184105 (2010).
16. J. Xu, J. Zhao, P. Korzhavyi, and B. Johansson, Comput Mater Sci 84, 301 (2014).
17. V. I. Razumovskiy, A. V. Ruban, and P. A. Korzhavyi, Phys Rev B 84, 024106 (2011).
18. J. S. Wróbel, D. Nguyen-Manh, M. Yu. Lavrentiev, M. Muzyk, and S. L. Dudarev, Phys Rev B 91, 024108 (2015).
19. A. V. Ponomareva, M. P. Belov, E. A. Smirnova, K. V. Karavaev, K. Sidnov, B. O. Mukhamedov, and I. A. Abrikosov, Phys Rev Mater 4, 094406 (2020).
20. W. Li, C. Xu, K. Chen, L. Liu, H. Yang, Q. Cheng, and M. Zeng, Coatings 12, 1588 (2022).
21. R. Idczak, R. Konieczny, T. Pikula, and Z. Surowiec, Corrosion 75 (2019).
22. A. M. Huntz, V. Bague, G. Beauplé, C. Haut, C. Sévérac, P. Lecour, X. Longaygue, and F. Ropital, Appl Surf Sci 207, 255 (2003).
23. S. Paul, M. Muralles, D. Schwen, M. Short, and K. Momeni, The Journal of Physical Chemistry C 125, 22863 (2021).
24. G. Kresse and D. Joubert, Phys Rev B 59, 1758 (1999).
25. P. E. Blöchl, Phys Rev B 50, 17953 (1994).
26. G. Kresse and J. Hafner, Phys Rev B 47, 558 (1993).
27. G. Kresse and J. Furthmüller, Phys Rev B 54, 11169 (1996).
28. G. Kresse and J. Furthmüller, Comput. Mater. Sci. 6, 15 (1996).
29. L. Vitos, Computational Quantum Mechanics for Materials Engineers, London, Springer-Verlag, London (2007). doi:10.1007/978-1-84628-951-4
30. L. Vitos, I. A. Abrikosov, and B. Johansson, Phys Rev Lett 87, 156401 (2001).
31. A. Zunger, S.-H. Wei, L. G. Ferreira, and J. E. Bernard, Phys Rev Lett 65, 353 (1990).
32. H. J. Monkhorst and J. D. Pack, Phys Rev B 13, 5188 (1976).
33. J. P. Perdew, K. Burke, and M. Ernzerhof, Phys Rev Lett 77, 3865 (1996).
34. J. von Pezold, A. Dick, M. Friák, and J. Neugebauer, Phys Rev B 81, 094203 (2010).
35. R. Hill, Proceedings of the Physical Society. Section A 65, 349 (1952).
36. J. Kollar, L. Vitos, and H. L. Skriver, Electronic Structure and Physical Properies of
37. Solids, Berlin, Heidelberg, Springer Berlin Heidelberg (2000).
38. A. V. Ruban and H. L. Skriver, Phys Rev B 66, 024201 (2002).
39. A. V. Ruban, S. Shallcross, S. I. Simak, and H. L. Skriver, Phys Rev B 70, 125115 (2004).
40. O. E. Peil, A. V. Ruban, and B. Johansson, Phys Rev B 85, 165140 (2012).
41. R. F. W. Bader, Acc Chem Res 18, 9 (1985).
42. E. Sanville, S. D. Kenny, R. Smith, and G. Henkelman, J Comput Chem 28, 899 (2007).
43. A. V. Ruban and M. Dehghani, Phys Rev B 94, 104111 (2016).
44. C. Wolverton and D. de Fontaine, Phys Rev B 49, 8627 (1994).
45. R. Idczak, R. Konieczny, and J. Chojcan, Acta Phys Pol A 129 (2016).
46. J. M. Cowley, J Appl Phys 21, 24 (1950).

47. A. V. Ponomareva, A. V. Ruban, O. Yu. Vekilova, S. I. Simak, and I. A. Abrikosov, Phys Rev B 84, 094422 (2011).
48. F. Ducastelle and F. Gautier, Journal of Physics F: Metal Physics 6, 2039 (1976).
49. I. Mirebeau, M. Hennion, and G. Parette, Phys Rev Lett 53, 687 (1984).
50. R. Idczak, R. Konieczny, and J. Chojcan, Solid State Commun 159 (2013).
51. O. I. Gorbatov, Y. N. Gornostyrev, A. R. Kuznetsov, and A. V. Ruban, Solid State Phenomena 172–174, 618 (2011).
52. A. L. Sutton and W. Hume-Rothery, The London, Edinburgh, and Dublin Philosophical Magazine and Journal of Science 46, 1295 (1955).
53. G. D. Preston, The London, Edinburgh, and Dublin Philosophical Magazine and Journal of Science 13, 419 (1932).
54. M. Ropo, K. Kokko, and L. Vitos, Phys Rev B 77, 195445 (2008).
55. E. P. Elsukov, G. N. Konygin, V. A. Barinov, and E. V. Voronina, Journal of Physics: Condensed Matter 4 (1992).
56. V. Niculescu, T. Litrenta, K. Raj, T. J. Burch, and J. I. Budnick, J Physical Soc Japan 42, 1538 (1977).
57. A. I. Liechtenstein, M. I. Katsnelson, V. P. Antropov, and V. A. Gubanov, J Magn. Magn. Mater. 67, 65 (1987).
58. M. Rahaman, B. Johansson, and A. V. Ruban, Phys Rev B 89, 064103 (2014).
59. G. R. Speich, A. J. Schwoeble, and W. C. Leslie, Metallurgical Transactions 3, 2031 (1972).
60. F. Mouhat and F.-X. Coudert, Phys Rev B 90, 224104 (2014).
61. S. F. Pugh, The London, Edinburgh, and Dublin Philosophical Magazine and Journal of Science 45 (1954).
62. J. Lee, T. Kim, I. S. Hwang, R. G. Ballinger, and J. H. Kim, Int. Conf. Fast React. Relat. Fuel Cycles 1 (2017).
63. R. Idczak, R. Konieczny, T. Pikula, and Z. Surowiec, Corrosion 75 (2019).